

# CANNYLINES: A PARAMETER-FREE LINE SEGMENT DETECTOR

Xiaohu Lu, Jian Yao<sup>†</sup>, Kai Li, and Li Li

School of Remote Sensing and Information Engineering, Wuhan University, P.R. China

<sup>†</sup>Email: jian.yao@whu.edu.cn Web: <http://cvrs.whu.edu.cn/>

## ABSTRACT

In this paper, we present a robust line segment detection algorithm to efficiently detect the line segments from an input image. Firstly a parameter-free Canny operator, named as *CannyPF*, is proposed to robustly extract the edge map from an input image by adaptively setting the low and high thresholds for the traditional Canny operator. Secondly, both efficient edge linking and splitting techniques are proposed to collect collinear point clusters directly from the edge map, which are used to fit the initial line segments based on the least-square fitting method. Thirdly, longer and more complete line segments are produced via efficient extending and merging. Finally, all the detected line segments are validated due to the Helmholtz principle [1, 2] in which both the gradient orientation and magnitude information are considered. Experimental results on a set of representative images illustrate that our proposed line segment detector, named as *CannyLines*, can extract more meaningful line segments than two popularly used line segment detectors, LSD [3] and EDLines [4], especially on the man-made scenes.

**Index Terms**— Line Segment Detector, Edge Map, Parameter-Free Canny, Line Segment Validation

## 1. INTRODUCTION

Line segment detection is an important and classical problem in image processing and computer vision. The line segments represent important geometric information of an image, especially when the scene of the image is comprised of many man-made objects. Besides, line segments can be used as low-level features to assist to solve problems such as stereo matching [5, 6], indoor scene layout recovering [7], simultaneous localization and mapping (SLAM) [8], road extraction [9], crack detection in materials, image compression, and so on.

In general, the line segment detection methods can be divided into two categories: gradient-orientation-based and gradient-magnitude-based. The idea of detecting line segments based on the gradient orientations was firstly proposed by Burns et al. [10] whose approach only depends on the gradient orientations. In contrast to classic line segment detectors based on the edge map, their proposed approach defines a line segment as a straight image region whose points share roughly the same image gradient orientation. A recently proposed line segment detector LSD [3] produces accurate line segments and controls the number of false detections in a low level by efficiently combing gradient orientations and the line validation according to the Helmholtz principle. The LSD states clearly what's an line segment, how to detect it and how to verify it, but the gradient magnitude threshold  $\rho$  is a safe threshold which eliminates some useful line information as well. Decreasing the value of  $\rho$  leads to detecting more but coarser line segments, which is an intrinsic problem of LSD because the gradient orientation is unstable when the gradient magnitude is small.

The gradient-magnitude-based methods first apply an edge detector to extract the edge map from the input image and then detect line segments based on the extracted edge map. Hough transform (HT) [11] is a traditional line detector based on an edge map, which extracts all lines containing a number of edge points exceeding a threshold. A lot of variants of the Hough transform have been proposed, e.g., the elliptical Gaussian kernel-based Hough transform [12], but they usually extract infinitely long lines instead of line segments and easily cause many false detections in richly-textured regions with strong edges. In order to overcome these shortcomings, Akinlar and Topal [4] proposed a robust and efficient line segment detector, named as EDLines, to extract line segments from edge segments, which consists of three main steps: 1) extracting the edge segments by the Edge Drawing (ED) [13] algorithm; 2) extracting line segments from the edge segments based on the least-square line fitting method; 3) eliminating false line segments according to the Helmholtz principle. The key problem of the edge segment based methods lies on that the line segment detection result suffers from the deficiency of the edge segment detection algorithm to a great extent. Even through EDPF [14] which is a parameter-free edge segment detector with a false detection control can get more reliable edge segments, a noisy point with strong gradient or a crossing of line segments can still deviate the edge segment's direction easily, thus a single linear edge segment can be detected as several short and curving segments. As a result, a longer line segment can be broken into several short ones, also the weak gradient parts of a line segment may be lost.

Actually, line segments should be detected directly from the image (e.g., LSD) or an edge map that contains all the structural information of the image, instead of the edge segments which has already lost some information in the edge segment detection. Following this thought, we propose a robust line segment detector, named as *CannyLines*, which extracts line segments based on an edge map obtained by applying a parameter-free Canny operator with the following contributions: 1) a parameter-free Canny operator, named as *CannyPF*, which adaptively chooses the low and high thresholds of the Canny operator for the input image by applying the Helmholtz Principle on the edge detection; 2) a line segment detector, which extracts the line segments directly based on edge map instead of edge segments; 3) a more reasonable validation step, which uses both the gradient orientation and magnitude information to verify each line segment.

## 2. ALGORITHM

In this section, we first give an overview of the proposed *CannyLines* algorithm, and then describe each step of the algorithm in detail. Given a grayscale image, the proposed *CannyLines* algorithm detects line segments via the following four steps: (1) *Edge map extraction*. A parameter-free Canny edge detector, named as *CannyPF*, is proposed to extract the edge map from an input image, which can self-adaptively adjust the low and high thresholds of the Canny oper-

ator based on the gradient magnitude of the input image, and which can ensure the completeness of the image's structure information. (2) *Edge linking and splitting*. Starting from the edge pixel with the greatest gradient magnitude, the linking process collects pixels on the edge map with a direction control. Therefore, an efficient splitting process is conducted to get short initial line segments. (3) *Line segments extending and merging*. The line segments are extended in both directions to collect more edge pixels and merged with other collinear line segments around. (4) *Line validation*. A novel line validation method based on the Helmholtz principle combining both gradient orientation and magnitude information is proposed to verify each line segment.

## 2.1. Parameter-Free Canny Operator

The standard Canny edge detector [15] consists of four steps [16]: (1) A Gaussian blur is applied to reduce image noise. (2) A gradient operator is applied to compute the magnitude and orientation of gradients. (3) Non-maximum suppression determines whether the pixel is a better candidate as an edge than its neighbors. (4) Hysteresis thresholding finds where edges begin and end. The Canny operator uses two thresholds instead of a single threshold, which makes it more flexible. However, the high threshold with a too high value can miss important information, on the other hand, the low threshold with a too low value will falsely identify irrelevant information (such as noise) as important. In fact, the two thresholds of Canny should not be set as a constant value for all the images, they should be adaptively adjusted according to the input image. Differing from the traditional Canny threshold selection method OTSU [17, 16] and the curve segments based edge detector [18], our proposed parameter-free Canny operator focuses on the completeness of the image's structural information after applying the Canny operator according to the Helmholtz principle.

### 2.1.1. Helmholtz Principle on Edge Detection

According to the computational Gestalt theory and the Helmholtz principle [1, 2], an observed geometric structure is perceptually "meaningful" if its number of occurrences would be very small in a random situation. In the work of Desolneux, Moisan and Morel (DMM) [19], the Helmholtz principle is used to define and compute edges and boundaries (closed edges) in an image by a parameter-free method. In our method, it is used to define the "minimal meaningful gradient magnitude" and the "maximal meaningless gradient magnitude", which are set as the low and high thresholds of the Canny operator.

Let  $\mathbf{I}$  be a discrete image of  $N \times N$  pixels,  $g(\mathbf{x})$  be the gradient magnitude at the pixel  $\mathbf{x}$  computed via finite differences,  $\mathbf{l}$  be a level line of the image  $\mathbf{I}$  with a length  $l$  counted in independent points. Then we consider the event:  $g(\mathbf{x}_i) \geq u$  for each pixel  $\mathbf{x}_i \in \mathbf{l}$ , i.e. each pixel of  $\mathbf{l}$  has a gradient magnitude larger than  $u$ . Since the  $l$  points are independent, the probability  $H(u)^l$  of this event is:

$$H(u)^l = \prod_{\mathbf{x}_i \in \mathbf{l}} P(g(\mathbf{x}_i) \geq u), \quad (1)$$

where  $H(u)$  is the probability for a point on any level line to have a contrast larger than  $u$ , which is defined as:

$$H(u) = \frac{1}{M} \#\{\mathbf{x} \in \mathbf{I} | g(\mathbf{x}) \geq u\}, \quad (2)$$

where  $M$  is the number of pixels of the image, whose gradient magnitudes are not equal to zero, i.e.,  $M = \#\{\mathbf{x} \in \mathbf{I} | g(\mathbf{x}) \neq 0\}$ . For each edge segment  $S_k$  with the length  $l_k$ , the number of connected

pieces of  $S_k$  is  $l_k \times (l_k - 1)/2$ , so the total number of connected pieces of all edge segments is computed as:

$$N_p = \sum_k l_k \times (l_k - 1)/2. \quad (3)$$

Considering a connected edge segment  $S$  with the length  $l$ , and with a minimum gradient magnitude  $u$  for the points in  $S$ , then the Number of False Alarms (NFA) of this event (edge segment) is defined as  $NFA(S) = N_p \times H(u)^l$ . Actually, NFA defines the number of false events (segment detections) under a reasonable noise model, which means the expectation of the number of segments like  $S$  output by the algorithm when run on a white-noise image.  $NFA(S) \leq 1$  represents the edge segment  $S$  is meaningful, otherwise, it is meaningless if  $NFA(S) > 1$ .

An intrinsic problem of the Helmholtz principle is that the meaningfulness of an "event" is considered in probability instead of in vision, which means that "if a significant part of a natural image happens to be very flat, as a consequence, all level lines long enough (with length larger than, say, 30 pixels) will be meaningful" [19] even their gradients is too low to be noticed in vision.

### 2.1.2. CannyPF

Following the thought of using the Helmholtz principle on edge detection, we introduce two new definitions according to the Helmholtz principle:

**Definition 1 - Minimal Meaningful Gradient Magnitude.** A gradient magnitude is defined as the minimal meaningful gradient magnitude  $g_{\min}$  if  $NFA(S_k) \leq 1$  for any edge segment  $S_k$  with a minimal gradient magnitude equal or greater than  $g_{\min}$ .

**Definition 2 - Maximal Meaningless Gradient Magnitude.** A gradient magnitude is defined as the maximal meaningless gradient magnitude  $g_{\max}$  if  $NFA(S_k) \geq 1$  for any edge segment  $S_k$  with a minimal gradient magnitude equal or less than  $g_{\max}$ .

The minimal length  $l_{\min}$  of all meaningful edge segments is determined by applying the Helmholtz principle on the gradient orientation, which is a constant value for an image calculated as:

$$l_{\min} = -4 \log(N) / \log(p), \quad (4)$$

where  $N$  is the bigger one of the width and height of the image, which is regarded as the maximal meaningful length  $l_{\max}$ , and  $p$  is a constant value for all the images which is set to 1/8 according to LSD [3]. Given any edge segment with the length in the range of  $[l_{\min}, l_{\max}]$ , *Definition 1* makes sure that it is meaningful if its minimum gradient magnitude is greater than  $g_{\min}$  and *Definition 2* ensures that it is meaningless if its minimum gradient magnitude is smaller than  $g_{\max}$ . As we have discussed above,  $g_{\max}$  is calculated in probability, the value of which varies from ten to hundreds. To balance the effects of probability and vision, we introduce a vision-meaningful parameter  $\lambda_v$  which denotes the lower limit of a gradient magnitude that is sufficient enough to be noticed in vision. Thus  $g_{\max}$  is revised as  $g_{\max} = \sqrt{\lambda_v} / g_{\max} \times g_{\max}$ . Algorithm 1 describes the procedure in details of our proposed parameter-free Canny operator in which the low and high thresholds for the traditional Canny operator *CannyPF* is adaptively computed based on the input image.

## 2.2. Edge Linking and Splitting

Based on the edge map obtained by the CannyPF operator, we apply the linking and splitting procedures used in the kernel-based Hough Transform (KHF) voting scheme [12], which is a simple but efficient way to obtain a large amount of edge segments containing nearly collinear edge points in the following three steps: (1) *Sorting*: all

---

**Algorithm 1** Parameter-Free Canny Edge Detection

---

**Input:** The input image **I****Output:** The edge map **E**

- 1: Apply a Gaussian blur on **I** to reduce the noise.
  - 2: Calculate gradient magnitudes via the Sobel operator.
  - 3: Build the histogram  $\mathcal{H}$  of gradient magnitudes of all pixels with the bin step size of 1.
  - 4: Calculate the probability distribution  $P(i)$  of the  $i$ -th bin of  $\mathcal{H}$ ,  $i = 1, 2, \dots, N_h$  where  $N_h$  denotes the bin size of  $\mathcal{H}$ .
  - 5: Compute  $N_p = \sum_{i=1}^{N_h} (\mathcal{H}(i) \times (\mathcal{H}(i) - 1)/2)$  where  $\mathcal{H}(i)$  denotes the frequency of the  $i$ -th bin of  $\mathcal{H}$  and the minimal meaningful length  $l_{\min}$  with Eq. (4).
  - 6: Compute  $H(g_{\min}) = (1/N_p)^{\frac{1}{l_{\min}}}$  and  $H(g_{\max}) = (1/N_p)^{\frac{1}{l_{\max}}}$  based on the assumption  $NFA(S) = N_p \times H(u)^l = 1$ .
  - 7:  $p = 0$
  - 8: **for**  $i = N_h : -1 : 1$  **do**
  - 9:    $p = p + P(i)$
  - 10:   **if**  $p \geq H(g_{\min})$  **then**
  - 11:      $g_{\min} = i$
  - 12:   **end if**
  - 13:   **if**  $p \geq H(g_{\max})$  **then**
  - 14:      $g_{\max} = i$
  - 15:   **end if**
  - 16: **end for**
  - 17: Revise  $g_{\max} = \sqrt{\lambda_v/g_{\max}} \times g_{\max}$
  - 18: **E**  $\leftarrow$  CANNY(...,  $g_{\max}$ ,  $g_{\min}$ , ...)
- 

the edge points are quickly sorted according to their gradient magnitudes. (2) *Linking*: starting from the edge point with the greatest gradient magnitude, the linking process searches the eight-connected neighbor edge points on the edge map with an orientation control scheme, which makes sure only the neighbor edge point with a gradient orientation enough close to one of the current edge point would be accepted. According to LSD, the gradient orientation difference tolerance is set to  $\pi/8$  for all the images. After the linking process of an edge segment is terminated, the same linking process is applied on the remaining edge points. All the edge segments are collected in such an iterative scheme. (3) *Splitting*: Any edge segment with a length larger than some small threshold  $\theta_s$  will be splitted into two edge segments at the point with a maximal deviation larger than one pixel to the line formed by the two endpoints of the edge segment. In this way, the edge segments will possibly be iteratively splitted.

### 2.3. Line Segment Extending and Merging

After edge linking and splitting, we get a cluster of edge segments whose points are nearly collinear, which are fed to a least square fitting function to get a large amount of initial line segments. Therefore, the proposed extending and merging strategies are applied to get longer and more complete line segments. Given a line segment  $\mathcal{L}_i$ , we extend it from one of its endpoints along the line direction. First we project this endpoint onto the fitted line  $\mathbf{l}_i$  to get the projected point  $\mathbf{p}^r$  in the real domain, which is rounded to the nearest integer point  $\mathbf{p}$ . Second we collect at most three nearest points  $\{\mathbf{q}_k\}_{k=1}^K$  ( $K \leq 3$ ) in the eight neighborhood of  $\mathbf{p}$  orthometric to the line extending direction, whose distances  $\{d(\mathbf{q}_k, \mathbf{l}_i)\}$  to  $\mathbf{l}_i$  are not larger than 1 pixel, i.e.,  $d(\mathbf{q}_k, \mathbf{l}_i) \leq 1, k = 1, \dots, K$ . Third we sort  $\{\mathbf{q}_k\}_{k=1}^K$  according to their distances to  $\mathbf{l}_i$  in the increasing order and sequentially check whether there exists any edge point in the locations of these points. If some edge point is found, we accept it as an *extending hypothesis*, otherwise, we regard this case as a *gap*. During the extending process, if some edge point of another

line segment  $\mathcal{L}_j$  with the fitted line  $\mathbf{l}_j$  is met and the direction difference between  $\mathbf{l}_i$  and  $\mathbf{l}_j$  is less than a pre-defined threshold  $\theta_m$ , these two line segments will be merged into a single line segment if the fitting mean squared error based on the least square fitting method is not large than 1 pixel. In this way, we continue to extend the line segment  $\mathcal{L}_i$  until there are two *gaps* in 5 continuous extending operations. The extended line segment  $\mathcal{L}_i$  will be refitted when the number of extending hypothesis is larger than the minimal meaningful length  $l_{\min}$ . While one extending direction is terminated, we start another extending direction in the same way.

### 2.4. Line Validation

Since Desolneux et al. [19] came up with a general framework to deal with parameter thresholds in image analysis, the line validation has become a standard configuration of the line segment detectors including LSD and EDLines. Let  $\mathcal{L}$  be a segment of a length  $n$  with at least  $k$  points having their directions aligned with the line direction in an image of size  $N \times N$ , then the *Number of False Alarms (NFA)* of  $\mathcal{L}$  is defined as:

$$NFA(n, k) = N^4 \times \sum_{i=k}^n \binom{n}{i} p^i (1-p)^{n-i}, \quad (5)$$

where  $p$  is the probability that a point is aligned with a line segment which is set to  $1/8$  for constant according to LSD.

The validation process discussed above uses only the orientation information of the edge points because the gradient orientation is “the simplest local contrast invariant information” [2]. The shortcoming of using the gradient orientation only is that when the gradient magnitude is small, the gradient orientation is unstable. LSD solves this problem by using a gradient threshold to filter out noisy backgrounds. Under this condition, the LSD using only the gradient orientation information “fails especially in images where the background contains some white noise” [4]. However, it is obvious that a line segment with high gradient magnitudes is a stronger feature than that with low gradient magnitudes when they share the same length and the same number of aligned points. Inspired by the Helmholtz principle on edge detection, we come up with a new definition of *Number of False Alarms* which combines both  $NFA(n, k)$  and  $NFA(S)$  because a line segment is obtained from an edge segment, which is defined as:

$$\begin{aligned} NFA(\mathcal{L}) &= NFA(n, k) \times NFA(S) \\ &= N^4 \times \sum_{i=k}^n \binom{n}{i} p^i (1-p)^{n-i} \times N_p \times H(u)^n, \end{aligned} \quad (6)$$

where  $u$  denotes the minimum gradient magnitude of the points in  $S$  and  $N_p$  is the total number of connected pieces of all edge segments as in Eq. (3). The definition of  $NFA(\mathcal{L})$  states that the line segment with more aligned points and higher gradient magnitudes is more likely to be a Gestalt.

## 3. EXPERIMENTAL RESULTS

### 3.1. Parameters

The proposed line segment detector *CannyLines* is parameter-free because all the parameters related to the input image are determined by the image itself, while other parameters can be set the same for all the images, which are discussed as follows:

(1)  $\lambda_v$  for edge detection, which denotes the lower limit of a gradient magnitude that is sufficient enough to be noticed in vision. Actually, it is difficult to give an accurate value of  $\lambda_v$  directly, so we tested different values of  $\lambda_v$  on a large amount of images captured from different scenes, and found that  $\lambda_v = 70$  is a good balance of



**Fig. 1.** Comparison of *CannyLines* with ( (a), (c) ) and without ( (b), (d) ) the use of the parameter  $\lambda_v$  in *CannyPF*.

**Table 1.** Line segments detection results of LSD, EDLines and *CannyLines*.

Scenes	LSD			EDLines			CannyLines			
	$N$	$L$	$L/N$	$N$	$L$	$L/N$	$N$	$L$	$L/N$	
In door	1	864	30614.9	<b>35.4</b>	748	27631.2	<b>36.9</b>	642	26589.3	<b>41.4</b>
	2	530	21545.4	<b>40.7</b>	444	19647.3	<b>44.3</b>	397	19965.5	<b>50.3</b>
	3	469	16539.6	<b>35.3</b>	407	15869.3	<b>39.0</b>	443	17738.3	<b>40.0</b>
	4	215	12302.2	<b>57.2</b>	170	12027.1	<b>70.7</b>	203	14351.4	<b>70.7</b>
	5	627	19500.9	<b>31.1</b>	577	18271.4	<b>31.7</b>	485	18063.2	<b>37.2</b>
Out door	1	823	22023.8	<b>26.8</b>	591	18464.2	<b>31.2</b>	633	21181.7	<b>33.5</b>
	2	562	14753.8	<b>26.3</b>	499	15680.7	<b>31.4</b>	484	15590.7	<b>32.2</b>
	3	266	8981.9	<b>33.8</b>	257	8928.0	<b>34.7</b>	270	9251.7	<b>34.3</b>
	4	471	12900.4	<b>27.4</b>	416	10610.9	<b>25.5</b>	327	11819.3	<b>36.1</b>
	5	348	12425.9	<b>35.7</b>	322	11180.7	<b>34.7</b>	313	12228.3	<b>39.1</b>

completeness and cleanliness. Without the use of  $\lambda_v$ , the line segments detection result represents the image directly in probability, which may lead to false negatives (see Fig. 1 (b) ) in the high contrast image and false positives (see Fig. 1 (d) ) in the low contrast image.

(2)  $\theta_s$  for edge segment splitting, which represents the minimal length of an edge segment to be considered for splitting and equals twice of the possibly shortest edge segment. For an image with a certain size, the minimal meaningful length  $l_{\min}$  is decided in probability, so we set  $\theta_s = l_{\min}/2$  which means that the length of the shortest edge segment splitting is  $l_{\min}/4$ . For most images the value of  $l_{\min}$  approximately equals 12, thus the length of the shortest edge segment is 3.

(3)  $\theta_m$  for line segment merging, which is the maximal direction deviation tolerance of two close-direction line segments to be considered for merging. We simply set  $\theta_m = 2 \times \tan(2/l_{\min})$ , which can be explained based on the fact that the two close-direction line segments with the length  $l_{\min}$  and with 1-pixel deviation of all their endpoints will be considered for merging. The  $\theta_m$  is used to quickly exclude the line segments that can't be merged.

### 3.2. Evaluation on *CannyPF*

To a great extent, an edge-based line segment detector benefits from the good edge detection map extracted from the input image. To quantitatively evaluate the effectiveness of the proposed parameter-free Canny edge detector *CannyPF*, we tested it on the *YorkUrbanD-B* database [20], which contains a series of images of man-made buildings and the corresponding ground-truth line segments of each image. Ten indoor images and ten outdoor images were chosen to evaluate the precisions of *CannyPF* and the following four edge detection methods: *CannySR* [21], *CannySRPF* [21], *ED* [13], and *EDPF* [14], the codes of which are obtained from the Edge Drawing library [21]. Let  $\mathbf{E}$  is the binary edge map obtained by applying an edge detector on the input image  $\mathbf{I}$ . Based on the assumption that one pixel of a ground-truth line segment of  $\mathbf{I}$  can be identified when there exists edge point(s) of  $\mathbf{E}$  in its eight neighborhood, the precision  $p$  of an edge detector on an input image  $\mathbf{I}$  was defined as  $p = \sum_k N(\mathcal{L}_k) / \sum_k |\mathcal{L}_k|$  where  $|\mathcal{L}_k|$  denotes the length or size of the ground-truth line segment  $\mathcal{L}_k$  in  $\mathbf{I}$  and  $N(\mathcal{L}_k)$  denotes the number of edge points in  $\mathcal{L}_k$  successfully identified in  $\mathbf{E}$ . Fig. 2 shows the edge detection results on the indoor and outdoor scene images, from which we can observe that *CannyPF* extracted more ground-truth edge pixels than other edge detectors either in indoor

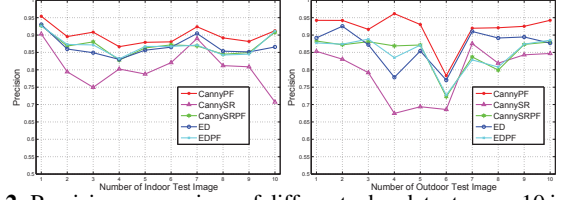


**Fig. 2.** Precision comparison of different edge detectors on 10 indoor scene images (Left) and 10 outdoor scene ones (Right).



**Fig. 3.** Line segments detection results of LSD ( $N = 898$ ,  $L/N = 56.5$ ), EDLines ( $N = 625$ ,  $L/N = 54.2$ ) and *CannyLines* ( $N = 823$ ,  $L/N = 108.1$ ) on an indoor image.

or in outdoor scene images, over which the average precision of the proposed *CannyPF* edge detector is 90.9%, which is obviously higher than 86.7% of *ED* and 85.9% of *EDPF*.

### 3.3. Evaluation on *CannyLines*

To evaluate the performance of the proposed line segment detector *CannyLines*, 5 indoor images and 5 outdoor ones were chosen from the tested images used in Section 3.2. Table 1 shows the statistical results of LSD, EDLines and *CannyLines*. As the amount of detected line segments can not reflect the effectiveness of a line segment detector very well, we use the average length of line segments to indicate the ability of different detectors. From Table 1, we can observe that on most images, the total line length  $L$  of the proposed *CannyLines* detector is longer than those of EDLines and close to those of LSD, and the average line length  $L/N$  is longer than those of LSD and EDLines, which means that the proposed *CannyLines* detector generated more meaningful line segments than LSD and EDLines generally. Fig. 3 is an intuitive demonstration of the performance of these three detectors on an indoor image. The execution programs of *CannyPF* and *CannyLines*, and more experimental results are available at <http://cvrs.whu.edu.cn/projects/cannyLines/>.

## 4. CONCLUSION

In this paper, we propose a robust line segment detector, named as *CannyLines*, which is based on the edge map obtained by applying a parameter-free Canny operator on the input image. A large amount of short edge segments containing nearly collinear points are collected via efficient edge linking and splitting operations on the edge map. The final line segments are obtained via fitting, extending, merging and validation from edge segments. The proposed *CannyLines* is parameter-free for all the input images. Experiments on representative images captured from different kinds of scenes examined the robustness and validity of our proposed parameter-free edge detector *CannyPF* and line segment detector *CannyLines*.

## Acknowledgment

This work was partially supported by the Natural Science Foundation of Hubei Province of China (Project No. 2013CFB296), the Hubei Province Science and Technology Support Program, China (Project No. 2015BAA027), the Jiangsu Province Science and Technology Support Program, China (Project No. BE2014866), and the South Wisdom Valley Innovative Research Team Program.

## 5. REFERENCES

- [1] Agnès Desolneux, Lionel Moisan, and Jean-Michel Morel, "Edge detection by Helmholtz principle," *Journal of Mathematical Imaging and Vision*, vol. 14, no. 3, pp. 271–284, 2001.
- [2] Agnès Desolneux, Lionel Moisan, and Jean-Michel Morel, *From gestalt theory to image analysis: a probabilistic approach*, Springer, 2008.
- [3] R. Grompone von Gioi, Jeremie Jakubowicz, Jean-Michel Morel, and Gregory Randall, "LSD: A fast line segment detector with a false detection control," *IEEE Transactions on Pattern Analysis and Machine Intelligence*, vol. 32, no. 4, pp. 722–732, 2010.
- [4] Cuneyt Akinlar and Cihan Topal, "EDLines: A real-time line segment detector with a false detection control," *Pattern Recognition Letters*, vol. 32, no. 13, pp. 1633–1642, 2011.
- [5] Herbert Bay, Vittorio Ferraris, and Luc Van Gool, "Wide-baseline stereo matching with line segments," in *IEEE Computer Society Conference on Computer Vision and Pattern Recognition (CVPR)*, 2005.
- [6] Hyunwoo Kim and Sukhan Lee, "Simultaneous line matching and epipolar geometry estimation based on the intersection context of coplanar line pairs," *Pattern Recognition Letters*, vol. 33, no. 10, pp. 1349–1363, 2012.
- [7] Jun Chu, Anzheng GuoLu, Lingfeng Wang, Chunhong Pan, and Shiming Xiang, "Indoor frame recovering via line segments refinement and voting," in *IEEE International Conference on Acoustics, Speech and Signal Processing (ICASSP)*, 2013.
- [8] Thomas Lemaire and Simon Lacroix, "Monocular-vision based SLAM using line segments," in *IEEE International Conference on Robotics and Automation*, 2007.
- [9] Radu Stoica, Xavier Descombes, and Josiane Zerubia, "A Gibbs point process for road extraction from remotely sensed images," *International Journal of Computer Vision*, vol. 57, no. 2, pp. 121–136, 2004.
- [10] J. Brian Burns, Allen R. Hanson, and Edward M. Riseman, "Extracting straight lines," *IEEE Transactions on Pattern Analysis and Machine Intelligence*, vol. PAMI-8, no. 4, pp. 425–455, 1986.
- [11] John Illingworth and Josef Kittler, "A survey of the Hough transform," *Computer vision, graphics, and image processing*, vol. 44, pp. 87–116, 1988.
- [12] Leandro AF Fernandes and Manuel M Oliveira, "Real-time line detection through an improved Hough transform voting scheme," *Pattern Recognition*, vol. 41, no. 1, pp. 299–314, 2008.
- [13] Cihan Topal and Cuneyt Akinlar, "Edge Drawing: A combined real-time edge and segment detector," *Journal of Visual Communication and Image Representation*, vol. 23, no. 6, pp. 862C–872, 2012.
- [14] Cuneyt Akinlar and Cihan Topal, "EDPF: a real-time parameter-free edge segment detector with a false detection control," *International Journal of Pattern Recognition and Artificial Intelligence*, vol. 26, no. 1, 2012.
- [15] John Canny, "A computational approach to edge detection," *IEEE Transactions on Pattern Analysis and Machine Intelligence*, vol. PAMI-8, no. 6, pp. 679–698, 1986.
- [16] Ping Zhou, Wenjun Ye, Yaojie Xia, and Qi Wang, "An improved Canny algorithm for edge detection," *Journal of Computational Information Systems*, vol. 7, no. 5, pp. 1516–1523, 2011.
- [17] Nobuyuki Otsu, "A threshold selection method from gray-level histograms," *IEEE Transactions on System, Man, and Cybernetics*, vol. SMC-9, no. 1, pp. 62–66, 1979.
- [18] Lu Wang, Suya You, and Ulrich Neumann, "Supporting range and segment-based hysteresis thresholding in edge detection," in *IEEE International Conference on Image Processing (ICIP)*, 2008.
- [19] Agnès Desolneux, Lionel Moisan, and Jean-Michel Morel, "Meaningful alignments," *International Journal of Computer Vision*, vol. 40, no. 1, pp. 7–23, 2000.
- [20] Patrick Denis, James H Elder, and Francisco J Estrada, *Efficient edge-based methods for estimating Manhattan frames in urban imagery*, Springer, 2008.
- [21] C. Akinlar and C. Topal, "Edge drawing library," <http://ceng.anadolu.edu.tr/cv/EdgeDrawing/>.